Correlation energies for He isoelectronic sequence with Z=2-116 from four-component relativistic configuration interactions

Watanabe, Yoshihiro
Department of Chemistry, Faculty of Sciences, Kyushu University

Tatewaki, Hiroshi
Institute of Natural Sciences and Information Center, Nagoya City University

出版情報：The Journal of Chemical Physics. 123 (7), pp.074322-, 2005-08-24. AIP Publishing
バージョン：

RESEARCH ARTICLE | AUGUST 24 2005

Correlation energies for He isoelectronic sequence with $Z = 2$–116 from four-component relativistic configuration interactions

Yoshihiro Watanabe; Hiroshi Tatewaki

J. Chem. Phys. 123, 074322 (2005)
https://doi.org/10.1063/1.1998867

Correlation energies for He isoelectronic sequence with $Z=2–116$ from four-component relativistic configuration interactions

Yoshihiro Watanabe
Department of Chemistry, Faculty of Sciences, Kyushu University, Hakozaki, Fukuoka 812-8581, Japan

Hiroshi Tatewaki[a)]
Institute of Natural Sciences and Information Center, Nagoya City University, Nagoya, Aichi 467-8501, Japan

(Received 26 April 2005; accepted 14 June 2005; published online 24 August 2005)

The relativistic correlation energies (CEs) for the He isoelectronic sequence from $_2$He to $_{116}$Uuh were investigated using configuration-interaction (CI) calculations. We used a large universal-type Gaussian basis set, which gives accurate Dirac-Fock total energies for the ions under consideration. In contrast to nonrelativistic CEs, the relativistic CEs decrease monotonically with increasing nuclear charge, but the *p*-, *d*-, and *f*-partial CEs have a hump like the relativistic Hylleraas CI. © *2005 American Institute of Physics*. [DOI: 10.1063/1.1998867]

I. INTRODUCTION

Helium-type ions are the simplest systems in which electronic interactions play a substantial role. Define TE(correlated) and TE(RHF) as the total energies (TEs) calculated with electronic correlations included and by restricted Hartree-Fock (RHF). It has been clarified that the nonrelativistic correlation energy (CE) as

$$\mathrm{CE(nonrel)} = \mathrm{TE(nonrel{:}correlated)} - \mathrm{TE(RHF)} \qquad (1)$$

is almost constant for atoms heavier than $_6$C,[1–4] as shown in Fig. 1, where the present results are also included; CE(nonrel) is -0.0451 hartree for $_6$C and is -0.0466 hartree for $_{100}$Fm.[2–4] In this paper a Dirac-Coulomb Hamiltonian is assumed. The relativistic correlation energy is given analogously by

$$\mathrm{CE(rel)} = \mathrm{TE(rel{:}correlated)} - \mathrm{TE(DF)}, \qquad (2)$$

where DF denotes a Dirac-Fock calculation. In contrast, Pestka and Karwowski[5,6](PK) showed using relativistic Hylleraas-type functions that the relativistic CE has a strong Z dependence (see Fig. 1). They considered that the two-electron generalization of the one-electron exact kinetic balance condition is necessary to guarantee the bound properties of the Hamiltonian eigenvalues,[7,8] but these are represented by an infinite sequence of conditions and can never be fulfilled exactly.[5,6] PK state that "We cannot exclude that the behavior of the relativistic CE for very large Z (strong decrease with increasing Z) may be an artifact resulting from a slight departure of eigenvalue of Dirac-Coulomb (DC) Hamiltonian describing the ground state from Hylleraas-Undheim-Macdonald theorem[9,10] conditions." Since the spinors in a multiconfiguration Dirac-Fock (MCDF) equation satisfy the boundary conditions and kinetic balance, the calculated TEs should be free from the artificial errors as in the case of numerical Dirac-Fock (NDF),[11] where no artificial error occurs. Pestka, Tatewaki, and Karwowski (PTK) calculated relativistic CEs by MCDF.[12] As indicated in Fig. 1, the MCDF CE follows the relativistic Hylleraas CE, showing that the strong decrease in CE is not a calculational artifact. PTK have also shown that the partial CE from the $2p$ and $3d$ shells has an extremum like the Hylleraas CE, but the strong decrease in the *s*-partial CE surpasses these extrema, producing a monotonic decrease in the MCDF CE as shown in Fig. 1. Tatewaki and Noro[13] (TN) also calculated the relativistic CE employing the third-order Douglas-Kroll[14] (DK3) Hamiltonian.[15] They used a universal set consisting of $33s$, $28p$, $28d$, and $28f$ primitive Gaussian-type functions (pGTFs) for all ions with $Z=1–120$, and performed the full configuration-interaction (CI) calculation. Although the absolute value of the DK3 CEs is several times larger than those of the Hylleraas CEs, the qualitative behavior is similar, again confirming the relativistic results of the Hylleraas CI. Although it is now confirmed that the relativistic Hylleraas CE for large Z is a good model, two problems remain: (1) the MCDF CE decreases monotonically from $Z=1$ to 102, whereas Hylleraas CE does not, and (2) the absolute value of the MCDF CE overtakes the Hylleraas CE at $_{97}$Bk. In this work, we consider these two problems using four-component relativistic CI calculations.

II. METHOD OF CALCULATION

A. Nucleus model and basis set

PTK (Ref. 12) and TN (Ref. 13) used a point-charge model for the nucleus when performing MCDF and DK3 calculations, respectively. However, it is difficult to describe the behavior of spinors accurately near the nucleus in this model when the Gaussian expansion method is employed. We therefore use the uniformly charged sphere model. The radius of the sphere R is given, following Visscher and Dyall,[16,17] as

a)Electronic mail: htatewak@nsc.nagoya-cu.ac.jp

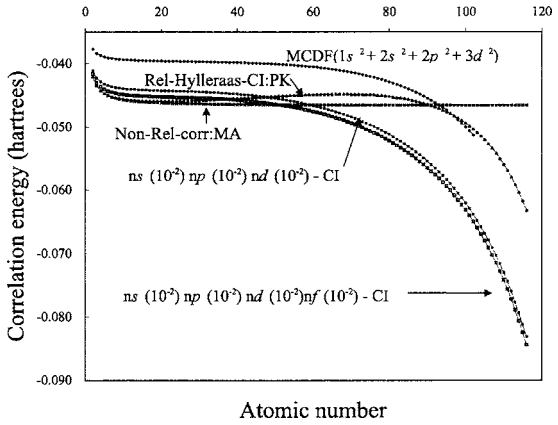

FIG. 1. The nonrelativistic (a) and relativistic correlation energies [(b)–(e)]. (a) Nonrelativistic correlation energies calculated by a $1/Z$ expansion given in Ref. 2. (b) Relativistic correlation energies calculated by MCDF given in Ref. 12. (c) Relativistic correlation energies calculated by Hylleraas CI given in Refs. 5 and 6. (d) Relativistic correlation energies calculated by $ns(10^{-2})np(10^{-2})nd(10^{-2})$-CI. (e) Estimated relativistic correlation energies by $ns(10^{-2})np(10^{-2})nd(10^{-2})nf(10^{-2})$-CI.

$$R = (2.039\,527\,14A^{1/3} + 1.390\,586\,68) \times 10^{-5}\ \text{bohr}, \quad (3)$$

where A is the mass number. Tatewaki and Watanabe[18,19] (TW) recently developed a universal GTF set accurate from $_1$H to $_{83}$Bi, where the exponent parameters are chosen to give the exact NDF TEs. The errors in TE are less than or equal to 0.000 001 hartree when

$$\begin{aligned} &58s_+58p\_58p_+36d\_36d_+36f\_36f_+ \\ &\quad \leqslant ns_+np\_np_+md\_md_+mf\_mf_+ \\ &\quad \leqslant 72s_+72p\_72p_+36d\_36d_+36f\_36f_+; \end{aligned}$$

here, the numbers before the symmetry l_i are the numbers of l_i pGTFs. We here used $62s_+$ below, and further made 68, 74, 80, 86, 92, 98, and 104 s_+ pGTF sets by adding primitives whose exponents are determined by the geometric sequence

$$\zeta_{n+1} = (\zeta_n/\zeta_{n-1})\zeta_n. \quad (4)$$

Table I gives the two-electron ion Dirac-Fock-Roothaan (DFR) TEs calculated for $_{60}$Nd, $_{80}$Hg, $_{100}$Fm, and $_{120}$Atom. In performing DFR calculations we used quadraprecision (16 bytes), and the accuracy of the total energy was 1×10^{-8} hartree. Almost perfect convergence occurred after $74s_+$ for all ions, indicating the completeness of these sets. For safety, hereafter, we used $80s_+$.

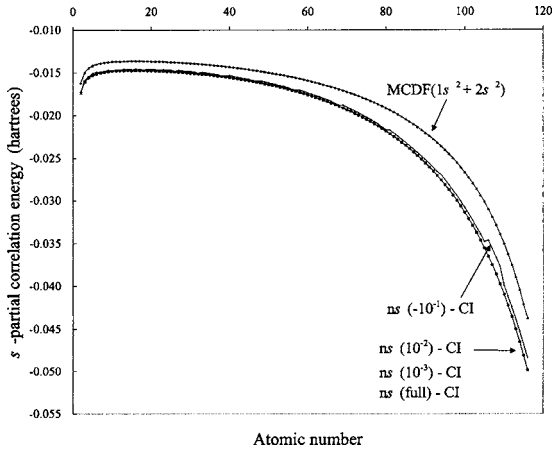

FIG. 2. The s-partial correlation energies (CE_s) given by MCDF ($1s^2 + 2s^2$), $ns(10^{-1})$-, $ns(10^{-2})$-, $ns(10^{-3})$-, and ns(full)-CI.

B. DFR and CI calculations

To find the relativistic CEs we first performed the DFR calculations. We then performed CI calculations using a relativistic CI code for linear molecules written by Watanabe and Matsuoka,[20,21] who noted that in linear molecules any single Slater determinant belongs to one of the irreducible representations of the $C_{\infty v}$ double group. The Slater-Condon rule[22–24] is directly used in this program to evaluate the matrix elements between the Slater determinants. Construction of correlating spinors is detailed in Sec. III.

III. RESULTS

We selected the atomic ions from $_2$He to $_{116}$Uuh, and used the mass numbers given by Visscher and Dyall from $_2$He to $_{102}$No and those given in the WebElements™ Periodic table[25] from $_{103}$Lr to $_{116}$Uuh, which were obtained experimentally.

A. *s*-partial correlation energies

We performed DFR and single and double excitation CI (SDCI) calculations using the occupied $1s_+$ and all the virtual (79) spinors. The calculated s-partial CE (hereafter denoted CE_s) is shown in Fig. 2 as the line labeled ns(full)-CI. The CE_s begins at -0.0174 hartree, has a maximum of -0.0147 hartree at $_{14}$Si and $_{15}$P, decreases gradually to ca. $_{80}$Hg, then sharply decreases as Z increases. It reaches -0.0499 hartree

TABLE I. Number of pGTF expansion terms and relativistic total energies relative to those (in hartree) by 104 expansion terms for Nd, Hg, Fm, and the $Z=120$ atom (the mass numbers for the respective atoms are given in parentheses). Relative energies are in microhartree.

pGTFs	$_{60}$Nd (142)	$_{80}$Hg (202)	$_{100}$Fm (257)	$_{120}$Atom (294)
62	0.49	−0.98	−3.57	82.58
68	0.01	−0.07	−0.20	7.97
74	0.00	−0.01	−0.04	0.39
80	0.00	−0.01	0.00	0.03
86	0.00	−0.01	0.00	0.01
92	0.00	−0.01	0.00	0.00
98	0.00	−0.01	0.00	0.00
104	−3750.519 155 15	−7002.455 714 92	−11 763.984 089 90	−18 973.261 226 40

at $_{116}$Uuh. To see whether ns(full)-CI gives the converged CE_ss, we performed CIs with pGTFs which have coefficients greater than 1×10^{-1}, 1×10^{-2}, and 1×10^{-3} in the $1s_+$ spinor, respectively, denoted as $ns(10^{-1})$, $ns(10^{-2})$, and $ns(10^{-3})$. Thus the CIs performed are

$$(s-1)ns(10^{-1})\text{-CI},$$

$$(s-2)ns(10^{-2})\text{-CI},$$

$$(s-3)ns(10^{-3})\text{-CI},$$

and

$$(s-4)ns(\text{full})\text{-CI}.$$

The numbers of pGTFs selected changes from one atom to another; the first threshold selects 4–6, the second 12–18, and the third 18–36 s_+ pGTFs. Prior to the CI calculations, we again performed DFR using the occupied $1s_+$ spinor, and selected pGTFs to prepare the virtual spinors for CI. The numbers of spinors thus generated were 5–7, 13–19, and 19–37 including the occupied $1s_+$ for the respective threshold, resulting in 25–49, 169–361, and 361–1369 configuration state functions (CSFs). The calculated CE_ss with the selected pGTFs are also shown in Fig. 2. We see that the $ns(10^{-2})$- and $ns(10^{-3})$-CIs give almost the same CE_ss as the ns(full)-CI: the CE_s errors with $ns(10^{-1})$-, $ns(10^{-2})$-, and $ns(10^{-3})$-CIs do not exceed 2×10^{-3}, 4×10^{-6}, and 0×10^{-6} hartree, respectively, relative to ns(full)-CI CE_s.

We know of no proof that CI calculations give the upper bound of the eigenvalue of the Dirac-Coulomb Hamiltonian. All the CE_ss, including that by MCDF, behave similarly as Z increases. Since the absolute value of CE_s increases in the order $ns(10^{-1})$-, $ns(10^{-2})$-, $ns(10^{-3})$-, and ns(full)-CI, and since $ns(10^{-2})$- and $ns(10^{-3})$-CIs give almost the same CE_ss as ns(full)-CI, we believe that ns(full)-CI gives exact CE_ss.

In the CI program the number of spinors is limited to 300, and we should therefore truncate the number of spinors. Hereafter we use s_+ pGTFs, selected using the threshold 10^{-2}, to calculate the partial CEs arising from the excitations to the higher l spinors, where a similar rule to s_+ is used for constructing the basis set: the rule, $nl_h(y\times10^{-1})$ selects the l_- and l_+ pGTFs having the same exponent as s_+ in $ns(y\times10^{-i})$.

B. *p*-partial correlation energies

Since we fix the threshold for s_+ as 10^{-2}, the number of s_+ spinors is in the range 13–19, including occupied $1s_+$. We prepared four p basis sets selected according to $np(10^{-1})$, $np(5\times10^{-2})$, $np(10^{-2})$, and $np(10^{-3})$, which involve using 4–6, 7–9, 12–18, and 18–36 pGTFs for p_- and p_+, respectively. The CIs performed are correspondingly denoted as

$$(p-1)ns(10^{-2})np(10^{-1})\text{-CI},$$

$$(p-2)ns(10^{-2})np(5\times10^{-2})\text{-CI},$$

$$(p-3)ns(10^{-2})np(10^{-2})\text{-CI},$$

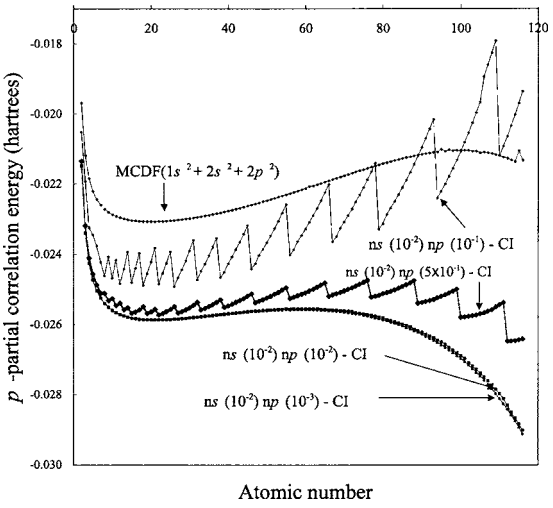

FIG. 3. The p-partial correlation energies (CE_p) given by MCDF ($1s^2+2s^2+2p^2$), $ns(10^{-2})np(10^{-1})$-, $ns(10^{-2})np(5\times10^{-2})$-, $ns(10^{-2})np(10^{-2})$-, and $ns(10^{-2})np(5\times10^{-3})$-CI.

and

$$(p-4)ns(10^{-2})np(10^{-3})\text{-CI}.$$

The numbers of resulting CSFs are, for example, 1513–3349 for $(p-2)$. The p-partial correlation CEs (CE_p) defined below are shown in Fig. 3;

$$\begin{aligned}&CE_p(ns(10^{-2})np(y\times10^{-i}))\\&\quad=\text{TE}(ns(10^{-2})np(y\times10^{-i})\text{-CI})-\text{TE}(ns(10^{-2})\text{-CI})\\&\quad(y=1\text{ or }5,\text{ and }i=1\text{–}4).\end{aligned}\tag{5}$$

We observed that all the CE_ps have humps. The threshold $ns(10^{-2})np(y\times10^{-i})$ introduces a number of ion groups having the same pGTFs; for example, there are 15 groups after $Z=7$ in $ns(10^{-2})np(10^{-1})$-CI. The CE_ps in the same group behave like a linear function of Z when the threshold is large, giving zigzag lines as shown in Fig. 3. The CE_p, according to MCDF($1s^2+2s^2+2p^2$) behaves like those by $ns(10^{-2})np(10^{-1})$-CI and $ns(10^{-2})np(5\times10^{-2})$-CI if we ignore the zigzag changes in the latter, indicating that a larger hump in MCDF arises from insufficiencies in the np^2 configurations.

The differences between $CE_p(ns(10^{-2})np(10^{-2})\text{-CI})$ and $CE_p(ns(10^{-2})np(10^{-3})\text{-CI})$ are always less than 0.000 15 hartree. We therefore infer that the CE_ps calculated with the two larger sets are correct, and that CE_p decreases at larger Z like CE_s.

Upon comparing CE_s and CE_p in Figs. 2 and 3 we see that calculated CE_ps (-0.0215–-0.0290 hartree) are as large as the CE_ss (-0.0147–-0.0499 hartree). The heights of the humps calculated with $ns(10^{-2})np(10^{-2})$-CI and $ns(10^{-2})np(10^{-3})$-CI are 0.000 32 and 0.000 30 hartree, several times smaller than by MCDF (0.002 06 hartree).

C. *d*-partial correlation energies

We have performed four series of CI calculations:

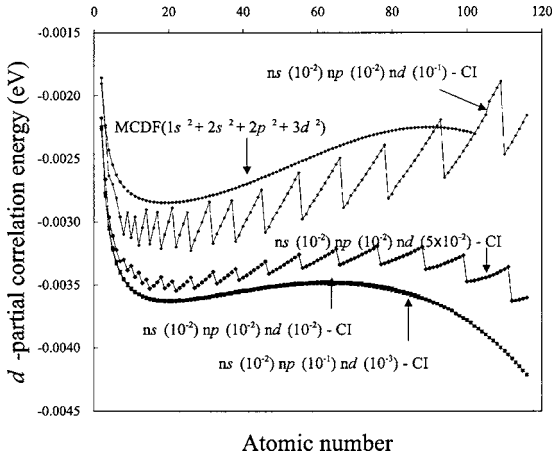

FIG. 4. The *d*-partial correlation energies (CE_d) given by MCDF ($1s^2+2s^2+2p^2+3d^2$), $ns(10^{-2})np(10^{-2})nd(10^{-1})$-, $ns(10^{-2})np(10^{-2})nd(5\times10^{-2})$-, $ns(10^{-2})np(10^{-2})nd(10^{-2})$-, and $ns(10^{-2})np(10^{-1})nd(10^{-3})$-CI.

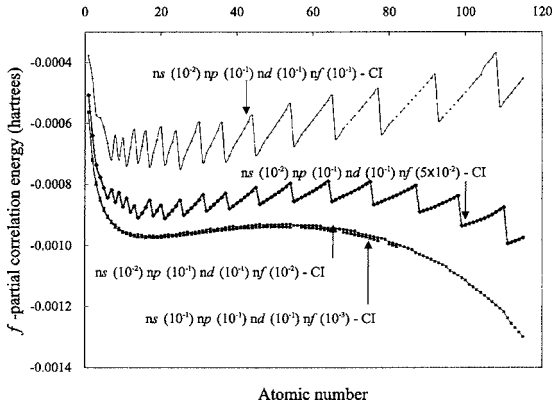

FIG. 5. The *f*-partial correlation energies (CE_f) given by $ns(10^{-2})np(10^{-1})nd(10^{-1})nf(10^{-1})$-, $ns(10^{-2})np(10^{-1})nd(10^{-1})nf(5\times10^{-2})$-, $ns(10^{-2})np(10^{-1})nd(10^{-1})nf(10^{-2})$-, and $ns(10^{-1})np(10^{-1})nd(10^{-1})nf(3.1\times10^{-3})$-CI.

$(d-1)ns(10^{-2})np(10^{-2})nd(10^{-1})$ - CI

from $_2$He to $_{116}$Uuh,

$(d-2)ns(10^{-2})np(10^{-2})nd(5\times10^{-2})$-CI

from $_2$He to $_{116}$Uuh,

$(d-3)ns(10^{-2})np(10^{-2})nd(10^{-2})$-CI

from $_2$He to $_{116}$Uuh,

and

$(d-4)ns(10^{-2})np(10^{-1})nd(10^{-3})$-CI

from $_2$He to $_{87}$Fr.

It was desirable to perform $ns(10^{-2})np(10^{-2})nd(10^{-3})$-CI, but the limit on the sizes of the basis set forces us to use $(d-4)$, where $np(10^{-1})$ is used instead of $np(10^{-2})$. The dimensions of the CIs are, for example, 5164–9754 for CI($ns(10^{-2})np(10^{-2})nd(10^{-2})$). The *d*-partial CEs ($CE_d$) defined by

$$\mathrm{CE}_d(ns(10^{-2})np(10^{-i})nd(y\times10^{-j})\text{-CI}) = \mathrm{TE}(ns(10^{-2})np(10^{-i})nd(y\times10^{-j})\text{ - CI}) - \mathrm{TE}(ns(10^{-2})np(10^{-i})\text{-CI}), \quad (6)$$

are shown Fig. 4. The large hump in CE_d calculated by MCDF again arises from inadequacies in the nd^2 configurations, as with CE_p. The $ns(10^{-2})np(10^{-1})nd(10^{-3})$-CI calculations give almost the same CE_ds as $ns(10^{-2})np(10^{-2})nd(10^{-2})$-CI; the former are 0.000 01–0.000 02 hartree lower than the latter. This indicates that (1) the CE_ds are almost independent of the sizes of the configurational space spanned by ns_+, np_-, and np_+ spinors, and (2) the CE_ds given by $ns(10^{-2})np(10^{-2})nd(10^{-2})$-CI are appropriate.

The calculated CE_ds (−0.0022–−0.0042 hartree) are one order smaller than the CE_ps (−0.0215–−0.0290 hartree). The height of the humps given by two larger sets takes the same value of 0.000 15 hartree, which is four times smaller than by MCDF (0.000 60 hartree).

D. *f*-partial correlation energies

Because of the limitation on the available pGTFs in the CI program, the following four CI calculations were performed:

$(f-1)ns(10^{-2})np(10^{-1})nd(10^{-1})nf(10^{-1})$-CI

from $_2$He to $_{116}$Uuh,

TABLE II. Partial and total CEs (hartree).

CE	$_2$He	Minimum	Z_{min}[a]	Maximum	Z_{max}[b]	Hump height	$_{116}$UuH
CE_s[c]	−0.017 351			−0.014 744	15,16		−0.049 865
CE_p[d]	−0.021 484	−0.025 862	20,21	−0.025 543	61–63	0.000 320	−0.029 011
CE_d[e]	−0.002 248	−0.003 625	20	−0.003 473	63	0.000 153	−0.004 248
CE_f[f]	−0.000 562	−0.000 970	17	−0.000 930	54–55	0.000 040	−0.001 299
Est-CE[g]	−0.041 644						−0.084 423

[a]The nuclear charge which gives minimum CE_i.
[b]The nuclear charge which gives maximum CE_i.
[c]Calculated from $ns(10^{-2})$-CI: see main text.
[d]Calculated from $ns(10^{-2})np(10^{-2})$-CI: see main text.
[e]Calculated from $ns(10^{-2})np(10^{-2})nd(10^{-2})$-CI: see main text.
[f]Calculated from $ns(10^{-2})np(10^{-1})nd(10^{-1})nf(10^{-2})$-CI: see main text.
[g]Est-CE is given by $CE_s+CE_p+CE_d+CE_f$.

TABLE III. DRF, $ns(10^{-2})np(10^{-2})nd(10^{-2})$-CI, and estimated $ns(10^{-2})np(10^{-2})nd(10^{-2})nf(10^{-2})$-CI total energies (in hartree).

Z	Mass	DRF	*nsnpnd*-CI	*nsnpndnf*-CI[a]	Z	Mass	DRF	*nsnpnd*-CI	*nsnpndnf*-CI[a]
2	4	−2.861 813	−2.902 896	−2.903 458	59	141	−3619.248 642	−3619.295 117 8	−3619.296 052
3	7	−7.237 205	−7.279 453	−7.280 170	60	142	−3750.519 155	−3750.565 768 8	−3750.566 704
4	9	−13.614 001	−13.656 851	−13.657 645	61	145	−3884.526 414	−3884.573 171 9	−3884.574 107
5	11	−21.993 148	−22.036 363	−22.037 208	62	152	−4021.297 867	−4021.344 774 6	−4021.345 710
6	12	−32.375 986	−32.419 446	−32.420 325	63	153	−4160.886 845	−4160.933 909 9	−4160.934 846
7	14	−44.764 194	−44.807 829	−44.808 732	64	158	−4303.307 609	−4303.354 864 0	−4303.355 806
8	16	−59.159 781	−59.203 548	−59.204 468	65	159	−4448.614 604	−4448.662 032 3	−4448.662 976
9	19	−75.565 082	−75.608 938	−75.609 871	66	164	−4596.825 128	−4596.872 737 6	−4596.873 682
10	20	−93.982 762	−94.026 702	−94.027 645	67	165	−4747.999 837	−4748.047 636 0	−4748.048 581
11	23	−114.415 814	−114.459 819	−114.460 773	68	166	−4902.168 618	−4902.216 614 2	−4902.217 561
12	24	−136.867 567	−136.911 619	−136.912 575	69	169	−5059.365 820	−5059.414 021 0	−5059.414 969
13	27	−161.341 675	−161.385 763	−161.386 723	70	174	−5219.632 834	−5219.681 249 2	−5219.682 199
14	28	−187.842 147	−187.886 277	−187.887 243	71	175	−5383.038 835	−5383.087 472 9	−5383.088 424
15	31	−216.373 308	−216.417 463	−216.418 429	72	180	−5549.596 468	−5549.645 337 8	−5549.646 291
16	32	−246.939 857	−246.984 033	−246.984 999	73	181	−5719.391 021	−5719.440 166 3	−5719.441 127
17	35	−279.546 804	−279.591 012	−279.591 982	74	184	−5892.443 862	−5892.493 262 4	−5892.494 226
18	40	−314.199 524	−314.243 749	−314.244 717	75	187	−6068.816 756	−6068.866 423 1	−6068.867 389
19	39	−350.903 830	−350.948 069	−350.949 037	76	192	−6248.550 399	−6248.600 342 5	−6248.601 311
20	40	−389.665 757	−389.710 022	−389.710 992	77	193	−6431.741 612	−6431.791 844 5	−6431.792 816
21	45	−430.491 724	−430.536 003	−430.536 972	78	195	−6618.416 486	−6618.467 019 7	−6618.467 994
22	48	−473.388 652	−473.432 945	−473.433 910	79	197	−6808.642 844	−6808.693 6912	−6808.694 667
23	51	−518.363 729	−518.408 034	−518.408 998	80	202	−7002.455 715	−7002.506 889 0	−7002.507 868
24	52	−565.424 609	−565.468 940	−565.469 906	81	205	−7199.965 449	−7200.017 000 5	−7200.017 989
25	55	−614.579 181	−614.623 527	−614.624 491	82	208	−7401.223 255	−7401.275 164 0	−7401.276 157
26	56	−665.835 953	−665.880 314	−665.881 275	83	209	−7606.325 106	−7606.377 389 1	−7606.378 386
27	59	−719.203 578	−719.247 955	−719.248 914	84	209	−7815.338 896	−7815.391 569 2	−7815.392 570
28	58	−774.691 529	−774.735 923	−774.736 879	85	210	−8028.317 348	−8028.370 428 0	−8028.371 433
29	63	−832.308 929	−832.353 355	−832.354 314	86	222	−8245.180 542	−8245.234 044 2	−8245.235 053
30	64	−892.066 367	−892.110 815	−892.111 771	87	223	−8466.345 401	−8466.399 345 9	−8466.400 359
31	69	−953.973 820	−954.018 290	−954.019 244	88	226	−8691.704 533	−8691.758 978 9	−8691.760 003
32	74	−1018.042 459	−1018.086 953	−1018.087 903	89	227	−8921.421 713	−8921.476 645 0	−8921.477 674
33	75	−1084.284 068	−1084.328 588	−1084.329 536	90	232	−9155.471 890	−9155.527 329 0	−9155.528 364
34	80	−1152.709 760	−1152.754 307	−1152.755 253	91	231	−9394.172 611	−9394.228 582 2	−9394.229 622
35	79	−1223.332 985	−1223.377 578	−1223.378 526	92	238	−9637.301 107	−9637.357 630 9	−9637.358 677
36	84	−1296.165 127	−1296.209 754	−1296.210 701	93	237	−9885.368 045	−9885.425 150 0	−9885.426 202
37	85	−1371.220 845	−1371.265 509	−1371.266 453	94	244	−10 138.052 555	−10 138.110 264 1	−10 138.111 321
38	88	−1448.513 123	−1448.557 825	−1448.558 767	95	243	−10 395.949 196	−10 396.007 541 2	−10 396.008 604
39	89	−1528.057 042	−1528.101 786	−1528.102 725	96	247	−10 658.777 592	−10 658.836 600 7	−10 658.837 670
40	90	−1609.867 216	−1609.912 005	−1609.912 942	97	247	−10 926.983 009	−10 927.042 766 5	−10 927.043 849
41	93	−1693.958 623	−1694.003 476	−1694.004 416	98	251	−11 200.397 788	−11 200.458 277 2	−11 200.459 368
42	98	−1780.347 158	−1780.392 063	−1780.393 002	99	252	−11 479.455 567	−11 479.516 827 2	−11 479.517 925
43	98	−1869.051 526	−1869.096 487	−1869.097 424	100	257	−11 763.984 091	−11 764.046 157 3	−11 764.047 263
44	102	−1960.086 284	−1960.131 303	−1960.132 239	101	258	−12 054.540 753	−12 054.603 668 7	−12 054.604 782
45	103	−2053.471 656	−2053.516 738	−2053.517 672	102	259	−12 351.106 873	−12 351.170 728 3	−12 351.171 856
46	106	−2149.224 342	−2149.269 490	−2149.270 422	103	262	−12 653.727 411	−12 653.792 207 0	−12 653.793 344
47	107	−2247.365 236	−2247.410 453	−2247.411 384	104	261	−12 962.995 381	−12 963.061 171 2	−12 963.062 317
48	114	−2347.910 197	−2347.955 507	−2347.956 442	105	262	−13 278.705 918	−13 278.772 753 2	−13 278.773 909
49	115	−2450.885 987	−2450.931 377	−2450.932 311	106	266	−13 600.938 897	−13 601.006 828 3	−13 601.007 994
50	120	−2556.308 409	−2556.353 883	−2556.354 815	107	264	−13 930.709 165	−13 930.778 260 6	−13 930.779 436
51	121	−2664.204 540	−2664.250 102	−2664.251 035	108	269	−14 267.033 698	−14 267.104 009 9	−14 267.105 196
52	130	−2774.588 584	−2774.634 239	−2774.635 171	109	268	−14 611.459 047	−14 611.530 654 3	−14 611.531 851
53	127	−2887.499 699	−2887.545 452	−2887.546 383	110	271	−14 963.166 030	−14 963.238 996 7	−14 963.240 203
54	132	−3002.946 288	−3002.992 143	−3002.993 073	111	272	−15 323.121 751	−15 323.196 159 9	−15 323.197 378
55	133	−3120.964 196	−3121.010 158	−3121.011 088	112	285	−15 689.589 004	−15 689.664 983 1	−15 689.666 221
56	138	−3241.571 633	−3241.617 731	−3241.618 665	113	284	−16 066.617 104	−16 066.694 762 3	−16 066.696 018
57	139	−3364.804 634	−3364.850 852	−3364.851 786	114	289	−16 451.562 500	−16 451.641 864 9	−16 451.643 135
58	140	−3490.687 227	−3490.733 571	−3490.734 506	115	288	−16 846.802 860	−16 846.884 059 3	−16 846.885 343
					116	292	−17 250.672 556	−17 250.755 680 9	−17 250.756 980

[a]Estimated value. See main text.

$(f-2)ns(10^{-2})np(10^{-1})nd(10^{-1})nf(5\times10^{-2})$-CI from $_2$He to $_{116}$Uuh,

$(f-3)ns(10^{-2})np(10^{-1})nd(10^{-1})nf(10^{-2})$-CI from $_2$He to $_{111}$Rg,

$(f-4)ns(10^{-1})np(10^{-1})nd(10^{-1})nf(10^{-2})$-CI from $_{110}$Ds to $_{116}$Uuh,

$(f-5)ns(10^{-1})np(10^{-1})nd(10^{-1})nf(3.1\times10^{-3})$-CI from $_2$He to $_{83}$Bi.

The f-partial CEs (CE_fs) are calculated in the same way as other partial CEs. The CE_fs for $_{110}$Ds and $_{111}$Rg calculated with $(f-4)$ are the same as those with $(f-3)$ up to six digits after the decimal point, indicating that CE_fs with $(f-4)$ can be used as substitutes for those with $(f-3)$. We used CE_fs calculated with $(f-4)$ for $_{112}$Uub–$_{116}$Uuh when treating CE_fs from $(f-3)$. Calculations with $(f-5)$ are performed to examine the CE convergence. The dimensions of the CIs are 5755–10 231 for $ns(10^{-2})np(10^{-1})nd(10^{-1})nf(10^{-2})$-CI, and the calculated CE_fs are given in Fig. 5.

The CE_fs for the respective ions using the above sets are almost the same except for those with $(f-1)$ and $(f-2)$; if we choose a certain ion, the order of the CE_f is always $|CE_f(f-3)|\leqslant|CE_f(f-5)|$. The difference between the two CEs is always less than 0.000 012 hartree, showing that $ns(10^{-2})np(10^{-1})nd(10^{-1})nf(10^{-2})$-CI gives appropriate f-partial CEs. The CE_fs (-0.0006–-0.0013 hartree) are several times smaller than the CE_ds (-0.0022–-0.0042 hartree). The height of the hump in the CE_fs given by the larger sets is 0.000 04 hartree, one-fourth of that of the CE_ds.

IV. DISCUSSION

Table II sets out the minimum and maximum partial CEs. The TEs calculated according to $ns(10^{-2})np(10^{-2})nd(10^{-2})$-CI and the estimated-TEs from $ns(10^{-2})np(10^{-2})nd(10^{-2})nf(10^{-2})$-CI, which are equal to $TE(ns(10^{-2})np(10^{-2})nd(10^{-2})\text{-CI})+CE_f(ns(10^{-2})np(10^{-1})nd(10^{-1})nf(10^{-2})\text{-CI})$, are listed in Table III. We also show the (total) CEs in Fig. 1.

Table II shows that the CE_s has a maximum, and CE_p, CE_d, and CE_f have small humps as discussed previously. We see that the (total) CE decreases monotonically as the nuclear charge Z increases, since the decrease in the sum of the higher partial CEs overcomes the increase in CE_s for smaller Z; the decrease in CE_s overcomes the increase in higher-partial CEs for intermediate Z, and all the partial CEs decrease for larger Z (see Fig. 1). The behavior of the CE is explained as follows. For small Z, CE decreases in parallel with the nonrelativistic CE, because the relativistic effects in the Hamiltonian are small. For middle Z, relativistic effects reduce the electron charge cloud, which leads to larger $|CEs|$, but this is canceled out by increasing relativistic precorrelation effects[13] from the increase in Z, arising intrinsically from spinors consisting of small and large components, so keeping CE nearly constant. For large Z, further reduction in the charge distribution surpasses the relativistic precorrelation effects, causing a strong decrease in CE.

The present results confirm those determined by relativistic Hylleraas CI.[5,6] However, CE estimated by $ns(10^{-2})np(10^{-2})nd(10^{-2})nf(10^{-2})$-CI overtakes that from Hylleraas at $_{38}$Sr and that from CE by $ns(10^{-2})np(10^{-2})nd(10^{-2})$-CI at $_{48}$Cd. Although the nucleus models used in the relativistic Hylleraas calculation and the present work differ, we believe that the two models give almost identical CEs, especially for atoms with $Z\leqslant54$. Probably the use of the larger two-electron basis sets than by PK[5,6] brings the Hylleraas CI results closer to the present values.

We finally consider the error in the present calculation. Geometric extrapolation gave shortfalls of up to $-0.000\,00$, $-0.000\,16$, $-0.000\,02$, and $-0.000\,01$ hartree for CE_s, CE_p, CE_d, and CE_f because of the truncation in the s_+, p_-, p_+, d_-, d_+, f_-, and f_+ spinors, resulting in errors of not more than -0.0002 hartree in TEs estimated with $ns(10^{-2})np(10^{-2})nd(10^{-2})nf(10^{-2})$-CI. Geometric extrapolation also reveals -0.0006-hartree shortfalls at maximum from disregarding spinors with greater angular momentum than f. As a result, the estimated TEs in Table III are expected to be higher than the exact energies by not more than 0.001 hartree.

V. CONCLUSION

The relativistic correlation energies (CEs) for the He isoelectronic sequence from $_2$He to $_{116}$Uuh have been investigated by means of configuration-interaction (CI) calculations. The basis set for the CI calculations comprised the DFR $1s_+$ spinors plus pGTFs selected from $80s_+$, $80p_-$, $80p_+$, $80d_-$, $80d_+$, $80f_-$, and $80f_+$ pGTFs. In contrast to the results of relativistic Hylleraas CI, the (total) CEs decrease monotonically with increasing nuclear charge as MCDF. The present CE overtakes the Hylleraas CE at $_{38}$Sr, confirming again the appropriateness of the MCDF results. The CE begins at -0.0416 hartree for $_2$He and ends at -0.0844 hartree with $_{116}$Uuh. The absolute values would be enlarged by not more than 0.001 hartree if we do not impose any restrictions on the spinors employed.

ACKNOWLEDGMENTS

Calculations were performed using IBM p650 processors in the Library and Information Processing Center of Nagoya City University. The present work is supported by a Grant-in-Aid from the Ministry of Education, Culture, Sport, Science, and Technology (MEXT) of Japan.

[1] E. Clementi, J. Chem. Phys. **38**, 2248 (1963).
[2] J. Midtdal and K. Aashanar, Phys. Norv. **2**, 99 (1967).
[3] G. W. Drake, Can. J. Phys. **66**, 586 (1988).
[4] E. R. Davidson, S. A. Hagstrom, and S. J. Chakravorty, Phys. Rev. A **44**, 7071 (1991).
[5] G. Pestka, Ph.D. thesis, Nicolaus Copernicus University, Torun, 2000.
[6] G. Pestka and J. Karwowski, in *Explicitly Correlated Wavefunctions in Chemistry and Physics*, edited by J. Rychlewski (Kluwer Academic, Dordrecht, 2003), p. 331.
[7] G. Pestka, Phys. Scr. **68**, 254 (2003).
[8] G. Pestka, Phys. Scr. **69**, 203 (2004).

[9] E. A. Hylleraas and B. Undheim, Z. Phys. **65**, 759 (1930).
[10] J. K. L. McDonald, Phys. Rev. **43**, 830 (1933).
[11] I. P. Grant, in *Atomic, Molecular, and Optical Physics Handbook*, edited by G. W. F. Drake (AIP, New York, 1996), p. 258.
[12] G. Pestka, H. Tatewaki, and J. Karwowski, Phys. Rev. A **70**, 024501 (2004).
[13] H. Tatewaki and T. Noro, Chem. Phys. Lett. **399**, 480 (2004).
[14] M. Douglas and N. M. Kroll, Ann. Phys. (N.Y.) **82**, 89 (1974).
[15] T. Nakajima and K. Hirao, Chem. Phys. Lett. **329**, 511 (2000).
[16] L. Visscher and K. G. Dyall, http://www.chem.vu.nl/~visscher/FiniteNuclei/FiniteNuclei.htm
[17] L. Visscher and K. G. Dyall, At. Data Nucl. Data Tables **67**, 207 (1997).
[18] H. Tatewaki and Y. Watanabe, J. Comp. Chem. 24, 1823 (2003).
[19] H. Tatewaki and Y. Watanabe, J. Chem. Phys. **121**, 4528 (2004).
[20] Y. Watanabe, Ph. D. thesis, Kyushu University, 2002.
[21] Y. Watanabe and O. Matsuoka, J. Chem. Phys. **116**, 9585 (2002).
[22] J. C. Slater, Phys. Rev. **34**, 1293 (1929).
[23] E. U. Condon, Phys. Rev. **36**, 1121 (1930).
[24] A. Zabo and N. S. Ostlund, *Modern Quantum Chemistry* (Dover, New York, 1989).
[25] http://www.webelements.com/